9. Stamping Techniques for Micro- and Nanofabrication

Soft-lithographic techniques that use rubber stamps and molds provide simple means to generate patterns with lateral dimensions that can be much smaller than one micron and can even extend into the single nanometer regime. These methods rely on the use of soft elastomeric elements typically made out of the polymer poly(dimethylsiloxane). The first section of this chapter presents the fabrication techniques for these elements together with data and experiments that provide insights into the fundamental resolution limits. Next, several representative soft-lithography techniques based on the use of these elements are presented: (i) microcontact printing, which uses molecular 'inks' that form self-assembled monolayers, (ii) near- and proximity-field photolithography for producing two- and three-dimensional structures with subwavelength resolution features, and (iii) nanotransfer printing, where soft or hard stamps print single or multiple layers of solid inks with feature sizes down to 100 nm. The chapter concludes with descriptions of some device-level applications that highlight the patterning capabilities and potential commercial uses of these techniques.

9.1 **High-Resolution Stamps** 280
9.2 **Microcontact Printing** 282
9.3 **Nanotransfer Printing** 284
9.4 **Applications** 288
9.4.1 Unconventional Electronic Systems 288
9.4.2 Lasers and Waveguide Structures ... 293
9.5 **Conclusions** 295
References 295

There is considerable interest in methods that can be used to build structures that have micron or nanometer dimensions. Historically, research and development in this area has been driven mainly by the needs of the microelectronics industry. The spectacularly successful techniques that have emerged from those efforts – such as photolithography and electron beam lithography – are extremely well suited to the tasks for which they were principally designed: forming structures of radiation-sensitive materials (including photoresists or electron beam resists) on ultraflat glass or semiconductor surfaces. Significant challenges exist in adapting these methods for new emerging applications and areas of research that require patterning of unusual systems and materials, (including those in biotechnology and plastic electronics), structures with nanometer dimensions (below 50–100 nm), large areas in a single step (larger than a few square centimeters), or nonplanar (rough or curved) surfaces. These established techniques also have the disadvantage of high capital and operational costs. As a result, some of the oldest and conceptually simplest forms of lithography – embossing, molding, stamping, writing, and so on – are now being re-examined for their potential to serve as the basis for nanofabrication techniques that can avoid these limitations [9.1]. Considerable progress has been made in the last few years, mainly by combining these approaches or variants of them with new materials, chemistries, and processing techniques. This chapter highlights some recent advances in high-resolution printing methods, in which a "stamp" forms a pattern of "ink" on a surface that it contacts. It focuses on approaches whose capabilities, level of development, and demonstrated applications indicate a strong potential for widespread use, especially in areas where conventional methods are unsuitable.

Contact printing involves the use of an element with surface relief (the "stamp") to transfer material applied to its surface (the "ink") to locations on a substrate that it contacts. The printing press, one of the earliest manufacturable implementations of this approach, was introduced by Gutenberg in the fifteenth century. Since then, this general approach has been used almost exclusively for producing printed text or images with features that are one hundred microns or larger

in their smallest dimension. The resolution is determined by the nature of the ink and its interaction with the stamp and/or substrate, the resolution of the stamp, and the processing conditions that are used for printing or to convert the pattern of ink into a pattern of functional material. This chapter focuses on (1) printing techniques that are capable of micron and nanometer resolution, and (2) their use for fabricating key elements of active electronic or optical devices and subsystems. It begins with an overview of some methods for fabricating high-resolution stamps and then illustrates two different ways that these stamps can be used to print patterns of functional materials. Applications that highlight the capabilities of these techniques and the performances of systems that are constructed with them are also presented.

9.1 High-Resolution Stamps

The printing process can be separated into two parts: fabrication of the stamp and the use of this stamp to pattern features defined by the relief on its surface. These two processes are typically quite different, although it is possible in some cases to use patterns generated by a stamp to produce a replica of that stamp. The structure from which the stamp is derived, which is known as the "master", can be fabricated with any technique that is capable of producing well-defined structures of relief on a surface. This master can then be used directly as the stamp, or to produce stamps via molding or printing procedures. It is important to note that the technique for producing the master does not need to be fast or low in cost. It also does not need to possess many other characteristics that might be desirable for a given patterning task: it is used just once to produce a master, which is directly or indirectly used to fabricate stamps. Each one of these stamps can then be used many times for printing.

In a common approach for the high-resolution techniques that are the focus of this chapter, an established lithographic technique, such as one of those developed for the microelectronics industry, defines the master. Figure 9.1 schematically illustrates typical processes. Here, photolithography patterns a thin layer of resist onto a silicon wafer. Stamps are generated from this structure in one of two ways: by casting against this master, or by etching the substrate with the patterned resist as a mask. In the first approach, the master itself can be used multiple times to produce many stamps, typically using a light or heat-curable prepolymer. In the second, the etched substrate serves as the stamp. Additional stamps can be generated either by repeating the lithography and etching, or by using the original stamp to print replica stamps. For minimum lateral feature sizes that are greater than $\approx 1-2$ microns, contact- or proximity-mode photolithography with a mask produced by direct write photolithography represents a convenient method of fabricating the master. For features smaller than ≈ 2 microns, several different techniques can be used [9.2], including: (1) projection mode photolithography [9.3], (2) direct write electron beam (or focused

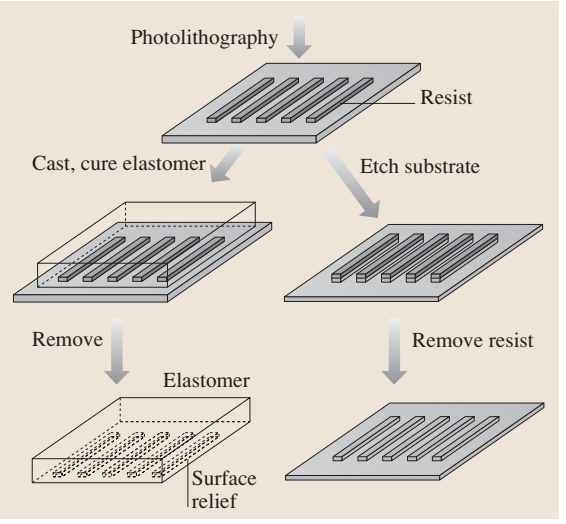

Fig. 9.1 Schematic illustration of two methods for producing high-resolution stamps. The first step involves patterning a thin layer of some radiation-sensitive material, known as the resist, on a flat substrate, such as a silicon wafer. It is convenient to use an established technique, such as photolithography or electron beam lithography, for this purpose. This structure, known as the 'master', is converted to a stamp either by etching or by molding. In the first case, the resist acts as a mask for etching the underlying substrate. Removing the resist yields a stamp. This structure can be used directly as a stamp to print patterns or to produce additional stamps. In the molding approach, a prepolymer is cast against the relief structure formed by the patterned resist on the substrate. Curing (thermally or optically) and then peeling the resulting polymer away from the substrate yields a stamp. In this approach, many stamps can be made with a single 'master' and each stamp can be used many times

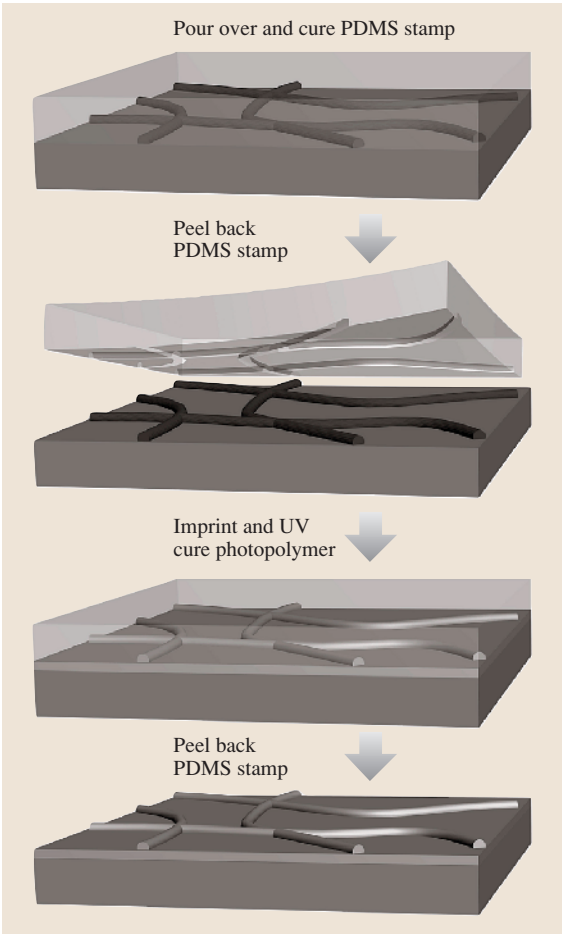

Fig. 9.2 Schematically illustrates a process for examining the ultimate limits in resolution of soft lithographic methods. The approach uses a SWNT master to create a PDMS mold with nanoscale relief features. Soft nanoimprint lithography transfers the relief on the PDMS to that on the surface of an ultraviolet curable photopolymer film

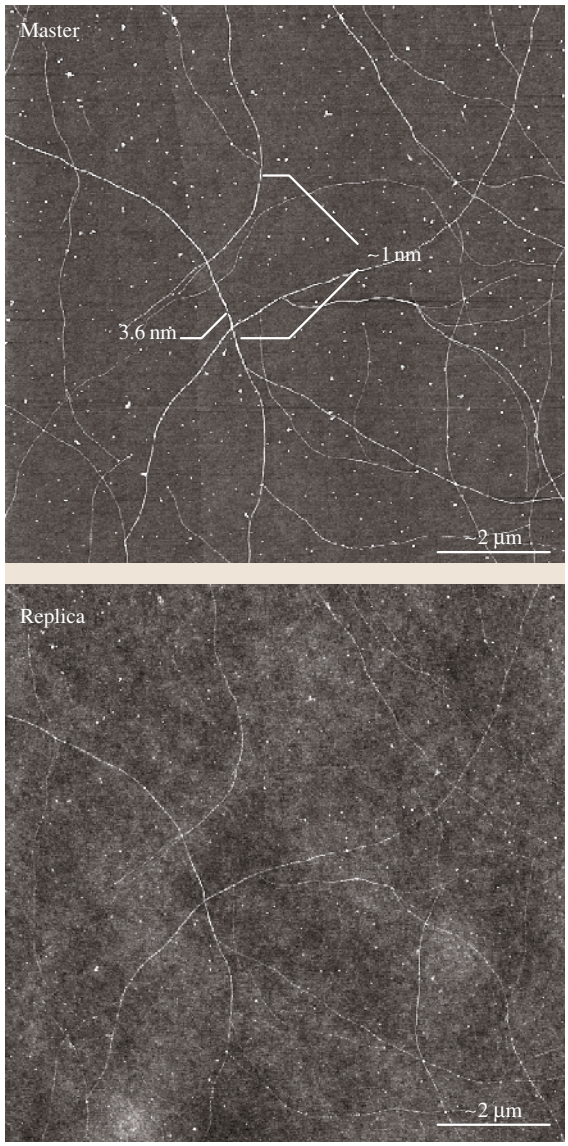

Fig. 9.3 Atomic force micrographs (*top* picture) of a "master" that consists of a submonolayer of single-walled carbon nanotubes (SWNTs; diameter between 0.5 and 5 nm) grown on a SiO_2/Si wafer. The *bottom* atomic force micrograph shows a replica of the relief structures in poly(urethane). These results indicate effective operation of a PDMS stamp for soft imprint lithography at the single nanometer scale

ion beam) lithography [9.4, 5], (3) scanning probe lithography [9.6–9] or (4) laser interference lithography [9.10]. The first approach requires a photomask generated by some other method, such as direct write photolithography or electron beam lithography. The reduction (typically 4×) provided by the projection optics relaxes the resolution requirements on the mask and enables features as small as ≈ 90 nm when deep ultraviolet radiation and phase shifting masks are used. The costs for these systems are, however, very high and their availability for general research purposes is limited. The second method is flexible in the geometry of patterns that can be produced, and the writing systems are highly developed: 30–50 nm features can be achieved with commercial systems [9.11], and < 10 nm features are possible with research tools, as first demonstrated

more than 25 years ago by *Broers* [9.12]. The main drawbacks of this method are that it is relatively slow and it is difficult to pattern large areas. Like projection-mode photolithography, it can be expensive. The third method, scanning probe lithography, is quite powerful in principle, but the tools are not as well established as those for other approaches. This technique has atomic resolution, but its writing speed can be lower and the areas that can be patterned are smaller than electron beam systems. Interference lithography provides a powerful, low-cost tool for generating periodic arrays of features with dimensions down to 100–200 nm; smaller sizes demand ultraviolet lasers, and patterns with aperiodic or nonregular features are difficult to produce.

In order to evaluate the ultimate resolution limit of the soft lithography methods, masters with relief structures in the single nanometer range must be fabricated. A simple method, presented in Fig. 9.2, uses submonolayer coverage of single-walled carbon nanotubes (SWNT grown, by established chemical vapor deposition techniques, on an ultraflat silicon wafer. The SWNT, which have diameters (heights and widths) in the 0.5–5 nm range, are molded on the bottom surface of a PDMS stamp generated by casting and curing against this master. Such a mold can be used to replicate the relief structure into a variety of photocurable polymers in a kind of soft nanoimprinting technique [9.13–15]. A single mold can give exceedingly high resolution, approaching the single nanometer scale range (comparable to a few bond lengths in the polymer backbone), as can be seen in Fig. 9.3 [9.16]. These results demonstrate the extreme efficiency of the basic soft lithographic procedure for generating and using elastomeric elements. The ultimate limits are difficult to predict, due to substantial uncertainties surrounding the polymer physics and chemistry that dominates in the nanometer regime.

9.2 Microcontact Printing

Microcontact printing (μCP) [9.17] is one of several soft lithographic techniques – replica molding, micromolding in capillaries, microtransfer molding, near-field conformal photolithography using an elastomeric phase-shifting mask, and so on – that have been developed as alternatives to established methods for micro- and nanofabrication [9.18–22]. μCP uses an elastomeric element (usually polydimethylsiloxane – PDMS) with high-resolution features of relief as a stamp to print patterns of chemical inks. It was mainly developed for use with inks that form self-assembled monolayers (SAMs) of alkanethiolates on gold and silver. The procedure for carrying out μCP in these systems is remarkably simple: a stamp, inked with a solution of alkanethiol, is brought into contact with the surface of a substrate in order to transfer ink molecules to regions where the stamp and substrate contact. The resolution and effectiveness of μCP rely on conformal contact between the stamp and the surface of the substrate, rapid formation of highly ordered monolayers [9.23], and the autophobicity of the SAM, which effectively blocks the reactive spreading of the ink across the surface [9.24]. It can pattern SAMs over relatively large areas (≈ up to 0.25 ft^2 has been demonstrated in prototype electronic devices) in a single impression [9.25]. The edge resolution of SAMs printed onto thermally evaporated gold films is on the order of 50 nm, as determined by lateral force microscopy [9.26]. Microcontact printing has been used with a range of different SAMs on various substrates [9.18]. Of these, alkanethiolates on gold, silver, and palladium [9.27] presently give the highest resolution. In many cases, the mechanical properties of the stamp limit the sizes of the smallest features that can be achieved: the most commonly used elastomer (Sylgard 184, Dow Corning) has a low modulus, which can lead to mechanical collapse or sagging for features of relief with aspect ratios greater than ≈ 2 or less than ≈ 0.05. Stamps fabricated with high modulus elastomers avoid some of these problems [9.28, 29]. Conventional stamps are also susceptible to in-plane mechanical strains that can cause distortions in the printed patterns. Composite stamps that use thin elastomer layers on stiff supports are effective at minimizing this source of distortion [9.30]. Methods for printing that avoid direct mechanical manipulation of the stamp can reduce distortions with conventional and composite stamps [9.25]. This approach has proven effective in large-area flexible circuit applications that require accurate multilevel registration.

The patterned SAM can be used either as a resist in selective wet etching or as a template in selective deposition to form structures of a variety of materials: metals, silicon, liquids, organic polymers and even biological species. Figure 9.4 schematically illustrates the use of μCP and wet etching to pattern a thin film of Au. Figure 9.5 shows SEM images of nanostructures of gold (20 nm thick, thermally evaporated with

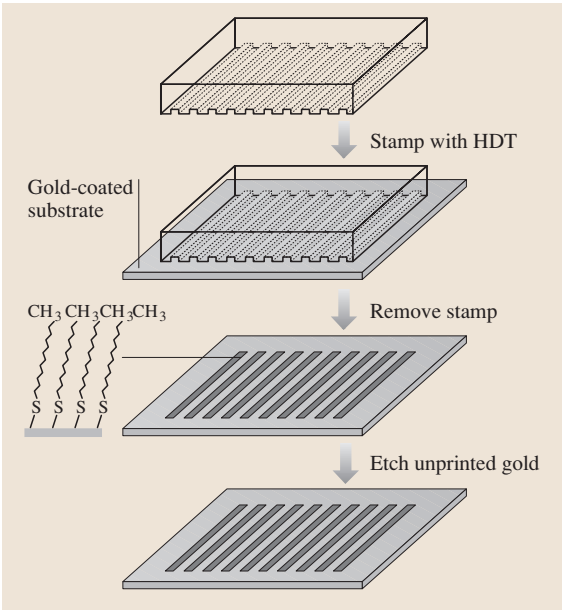

Fig. 9.4 Schematic illustration of microcontact printing. The first step involves "inking" a "stamp" with a solution of a material that is capable of forming a self-assembled monolayer (SAM) on a substrate that will be printed. In the case illustrated here, the ink is a millimolar concentration of hexadecanethiol (HDT) in ethanol. Directly applying the ink to the surface of the stamp with a pipette prepares the stamp for printing. Blowing the surface of the stamp dry and contacting it to a substrate delivers the ink to areas where the stamp contacts the substrate. The substrate consists of a thin layer of Au on a flat support. Removing the stamp after a few seconds of contact leaves a patterned SAM of HDT on the surface of the Au film. The printed SAM can act as a resist for the aqueous-based wet etching of the exposed regions of the Au. The resulting pattern of conducting gold can be used to build devices of various types

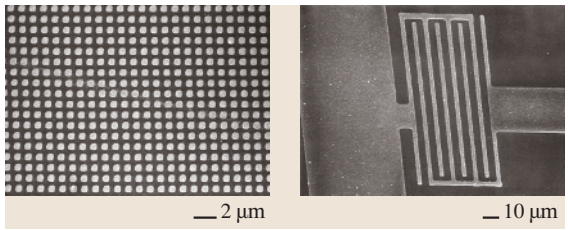

Fig. 9.5 Scanning electron micrographs of typical structures formed by microcontact printing a self-assembled monolayer ink of hexadecanethiol onto a thin metal film followed by etching of the unprinted areas of the film. The *left* frame shows an array of Au (20 nm thick) dots with ≈ 500 nm diameters. The *right* frame shows a printed structure of Ag (100 nm thick) in the geometry of interdigitated source/drain electrodes for a transistor in a simple inverter circuit. The edge resolution of patterns that can be easily achieved with microcontact printing is 50–100 nm

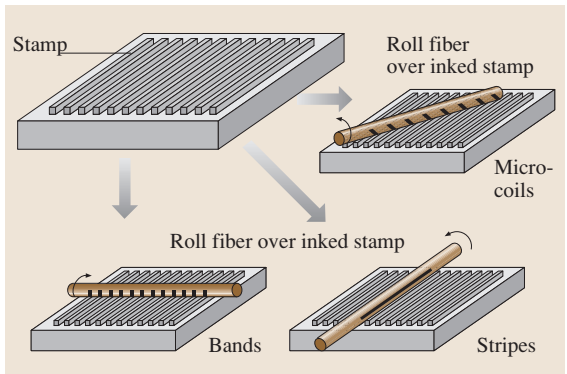

Fig. 9.6 Schematic illustration of a simple method to print lines on the surfaces of optical fibers. Rolling a fiber over the inked stamp prints a pattern onto the fiber surface. Depending on the orientation of the fiber axis with the line stamp illustrated here, it is possible, in a single rotation of the fiber, to produce a continuous microcoil, or arrays of bands or stripes

a 2.5 nm layer of Ti as an adhesion promoter) and silver (≈ 100 nm thick formed by electroless deposition using commercially available plating baths) [9.31] that were fabricated using this approach. In the first and second examples, the masters for the stamps consisted of photoresist patterned on silicon wafers with projection and contact mode photolithography, respectively. Placing these masters in a desiccator for ≈ 1 h with a few drops of tridecafluoro-1,1,2,2-tetrahydrooctyl-1-trichlorosilane forms a silane monolayer on the exposed native oxide of the silicon. This monolayer prevents adhesion of the master to PDMS (Sylgard 184), which is cast and cured from a 10:1 mixture of prepolymer and curing agent. Placing a few drops of a ≈ 1 mM solution of hexadecanethiol (HDT) in ethanol on the surface of the stamps and then blowing them dry with a stream of nitrogen prepares them for printing. Contacting the metal film for a few seconds with the stamp produces a patterned self-assembled monolayer (SAM) of HDT. An aqueous etchant (1 mM $K_4Fe(CN)_6$, 10 mM $K_3Fe(CN)_6$, and 0.1 M $Na_2S_2O_3$) removes the unprinted regions of the silver [9.32]. A similar solution (1 mM $K_4Fe(CN)_6$, 10 mM $K_3Fe(CN)_6$, 1.0 M KOH, and 0.1 M $Na_2S_2O_3$) can be used to etch the bare gold [9.33]. The

results in Fig. 9.5 show that the roughness on the edges of the patterns is ≈ 50–100 nm. The resolution is determined by the grain size of the metal films, the isotropic etching process, slight reactive spreading of the inks, and edge disorder in the patterned SAMs.

The structures of Fig. 9.5 were formed on the flat surfaces of silicon wafers (left image) and glass slides (right image). An attractive feature of μCP and certain other contact printing techniques is their ability to pattern features with high resolution on highly curved or rough surfaces [9.22, 34, 35]. This type of patterning task is difficult or impossible to accomplish with photolithography due to its limited depth of focus and the difficulty involved with casting uniform films of photoresist on nonflat surfaces. Figure 9.6 shows, as an example, a straightforward approach for high-resolution printing on the highly curved surfaces of optical fibers. Here, simply rolling the fiber over an inked stamp prints a pattern on the entire outer surface of the fiber. Simple staging systems allow alignment of features to the fiber axis; they also ensure registration of the pattern from one side of the fiber to the other [9.20]. Figure 9.7 shows 3 micron-wide lines and spaces printed onto the surface of a single mode optical fiber (diameter 125 μm). The bottom frame shows a freestanding metallic structure with the geometry and mechanical properties of an intravascular stent, which is a biomedical device that is commonly used in balloon angioplasty procedures. In this latter case μCP followed by electroplating generated the Ag microstructure on a sacrificial glass cylinder that was subsequently etched away with concentrated hydrofluoric acid [9.36]. Other examples of microcontact printing on nonflat surfaces (low cost plastic sheets and optical ridge waveguides) appear in the *Applications* section of this chapter.

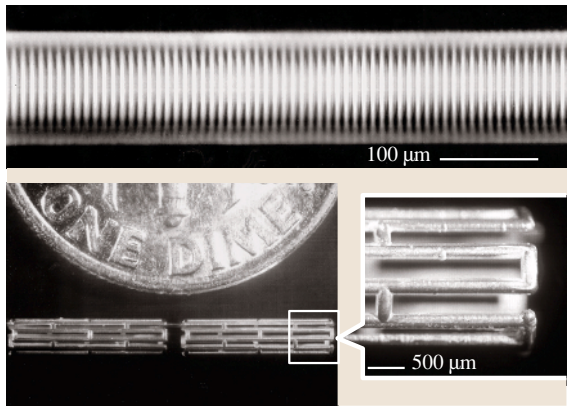

Fig. 9.7a–c Optical micrographs of some three-dimensional microstructures formed by microcontact printing on curved surfaces. The *top* frame shows an array of 3 micron lines of Au (20 nm)/Ti (1.5 nm) printed onto the surface of an optical fiber. This type of structure can be used as an integrated photomask for producing mode-coupling gratings in the core of the fiber. The *bottom* frames show a free-standing metallic microstructure formed by **(a)** microcontact printing and etching a thin (100 nm thick) film of Ag on the surface of a glass microcapillary tube, **(b)** electroplating the Ag to increase its thickness (to tens of microns) and **(c)** etching away the glass microcapillary with concentrated hydrofluoric acid. The structure shown here has the geometry and mechanical properties of an intravascular stent, which is a biomedical device commonly used in balloon angioplasty

9.3 Nanotransfer Printing

Nanotransfer printing (nTP) is a more recent high-resolution printing technique, which uses surface chemistries as interfacial "glues" and "release" layers (rather than "inks", as in μCP) to control the transfer of solid material layers from relief features on a stamp to a substrate [9.37–39]. This approach is purely additive (material is only deposited in locations where it is needed), and it can generate complex patterns of single or multiple layers of materials with nanometer resolution over large areas in a single process step. It does not suffer from surface diffusion or edge disorder in the patterned inks of μCP, nor does it require post-printing etching or deposition steps to produce structures of functional materials. The method involves four components: (1) a stamp (rigid, flexible, or elastomeric) with relief features in the geometry of the desired pattern, (2) a method for depositing a thin layer of solid material onto the raised features of this stamp, (3) a means of bringing the stamp into intimate physical contact with a substrate, and (4) surface chemistries that prevent adhesion of the deposited material to the stamp and promote its strong adhesion to the substrate. nTP has been demonstrated with SAMs and other surface chemistries for printing onto flexible and rigid substrates with hard inorganic and soft polymer stamps. Figure 9.8 presents a set of procedures for using nTP to pattern a thin metal

bilayer of Au/Ti with a surface transfer chemistry that relies on a dehydration reaction [9.37]. The process begins with fabrication of a suitable stamp. Elastomeric stamps can be built using the same casting and curing procedures described for μCP. Rigid stamps can be fabricated by (1) patterning resist (such as electron beam resist or photoresist) on a substrate (such as Si or GaAs), (2) etching the exposed regions of the substrate with an anisotropic reactive ion etch, and (3) removing the resist, as illustrated in Fig. 9.1. For both types of stamps, careful control of the lithography and the etching steps yields features of relief with nearly vertical or slightly re-entrant sidewalls. The stamps typically have depths of relief $> 0.2\,\mu m$ for patterning metal films with thicknesses $< 50\,nm$.

Electron beam evaporation of Au (20 nm; 1 nm/s) and Ti (5 nm; 0.3 nm/s) generates uniform metal bilayers on the surfaces of the stamp. A vertical, collimated flux of metal from the source ensures uniform deposition only on the raised and recessed regions of relief. The gold adheres poorly to the surfaces of stamps made of GaAs, PDMS, glass, or Si. In the process of Fig. 9.8, a fluorinated silane monolayer acts to reduce the adhesion further when a Si stamp (with native oxide) is used. The Ti layer serves two purposes: (1) it promotes adhesion between the Au layer and the substrate after pattern transfer, and (2) it readily forms a ≈ 3 nm oxide layer at ambient conditions, which provides a surface where the dehydration reaction can take place. Exposing the titanium oxide (TiO_x) surface to an oxygen plasma breaks bridging oxygen bonds, thus creating defect sites where water molecules can adsorb. The result is a titanium oxide surface with some fractional coverage of hydroxyl (−OH) groups (titanol).

In the case of Fig. 9.8, the substrate is a thin film of PDMS (10–50 μm thick) cast onto a sheet of poly(ethylene terephthalate) (PET; 175 μm thick). Exposing the PDMS to an oxygen plasma produces surface (−OH) groups (silanol). Placing the plasma-oxidized, Au/Ti-coated stamp on top of these substrates leads to intimate, conformal contact between the raised regions of the stamp and the substrate, without the application of any external pressure. (The soft, conformable PDMS is important in this regard.) It is likely that a dehydration reaction takes place at the (−OH)-bearing interfaces during contact; this reaction results in permanent Ti−O−Si bonds that produce strong adhesion between the two surfaces. Peeling the substrate and stamp apart transfers the Au/Ti bilayer from the raised regions of the stamp (to which the metal has extremely poor adhesion) to the substrate. Complete pattern transfer from an elastomeric

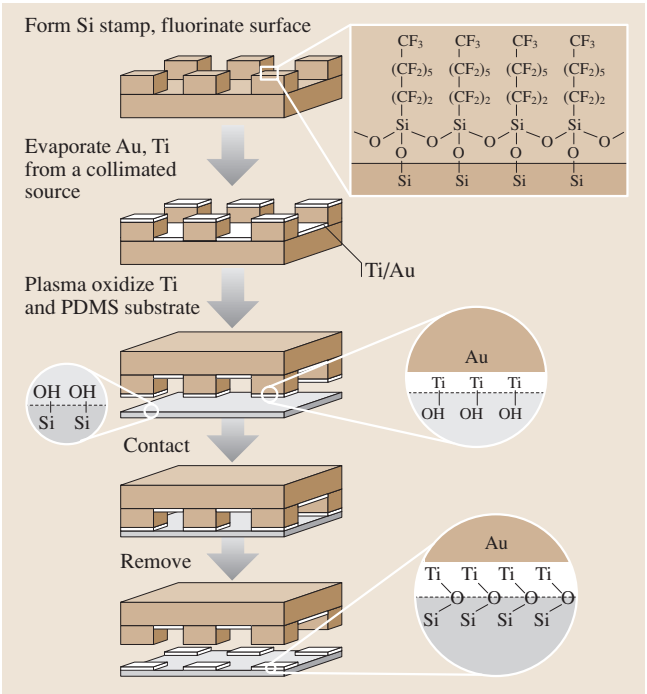

Fig. 9.8 Schematic illustration of nanotransfer printing procedure. Here, interfacial dehydration chemistries control the transfer of a thin metal film from a hard inorganic stamp to a conformable elastomeric substrate (thin film of polydimethylsiloxane (PDMS) on a plastic sheet). The process begins with fabrication of a silicon stamp (by conventional lithography and etching) followed by surface functionalization of the native oxide with a fluorinated silane monolayer. This layer ensures poor adhesion between the stamp and a bilayer metal film (Au and Ti) deposited by electron beam evaporation. A collimated flux of metal oriented perpendicular to the surface of the stamp avoids deposition on the sidewalls of the relief. Exposing the surface Ti layer to an oxygen plasma produces titanol groups. A similar exposure for the PDMS produces silanol groups. Contacting the metal-coated stamp to the PDMS results in a dehydration reaction that links the metal to the PDMS. Removing the stamp leaves a pattern of metal in the geometry of the relief features

stamp to a thin elastomeric substrate occurs readily at room temperature in open air with contact times of less than 15 seconds. When a rigid stamp is employed, slight heating is needed to induce transfer. While the origin of this difference is unclear, it may reflect the comparatively poor contact when rigid stamps are used; similar differences are also observed in cold welding of gold films [9.40].

Figure 9.9 shows scanning electron micrographs of a pattern produced using a GaAs stamp generated by

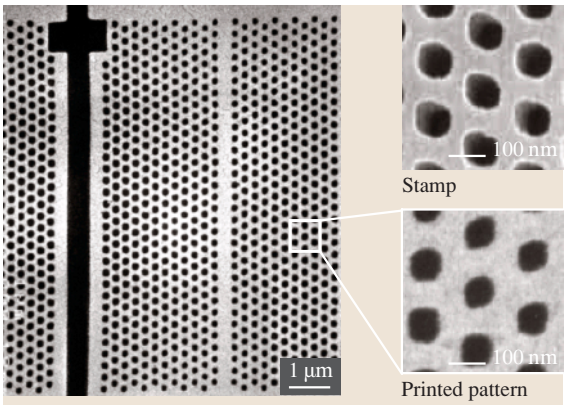

Fig. 9.9 Scanning electron micrograph (SEM) of a pattern produced by nanotransfer printing. The structure consists of a bilayer of Au(20 nm)/Ti (1 nm) (*white*) in the geometry of a photonic bandgap waveguide printed onto a thin layer of polydimethylsiloxane on a sheet of plastic (*black*). Electron beam lithography and etching of a GaAs wafer produced the stamp that was used in this case. The transfer chemistry relied on condensation reactions between titanol groups on the surface of the Ti and silanol groups on the surface of the PDMS. The frames on the *right* show SEMs of the Au/Ti-coated stamp (*top*) before printing and on the substrate (*bottom*) after printing. The electron beam lithography and etching used to fabricate the stamp limit the minimum feature size (≈ 70 nm) and the edge resolution (≈ 5–10 nm) of this pattern

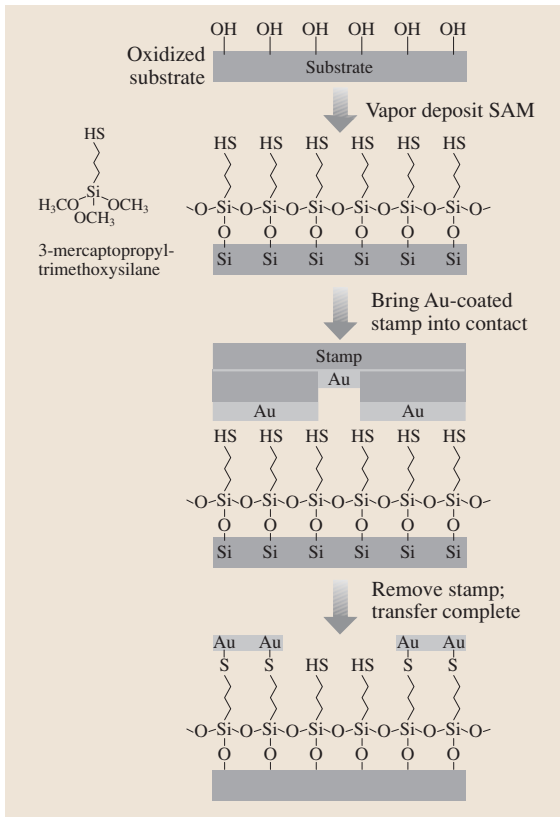

Fig. 9.10 Schematic illustration of steps involved in nanotransfer printing a pattern of a thin layer of Au onto a silicon wafer using a self-assembled monolayer (SAM) surface chemistry. Plasma oxidizing the surface of the wafer generates OH groups. Solution or vapor phase exposure of the wafer to 3-mercaptopropyltrimethoxysilane yields a SAM with exposed thiol groups. Contacting an Au-coated stamp to this surface produces thiol linkages that bond the gold to the substrate. Removing the stamp completes the transfer printing process

electron beam lithography and etching. The frames on the right show images of the metal-coated stamp before printing (top) and the transferred pattern (bottom). The resolution appears to be limited only by the resolution of the stamp itself, and perhaps by the grain size of the metal films. Although the accuracy in multilevel registration that is possible with nTP has not yet been quantified, its performance is likely similar to that of embossing techniques when rigid stamps are used [9.41].

A wide range of surface chemistries can be used for the transfer. SAMs are particularly attractive due to their chemical flexibility. Figure 9.10 illustrates the use of a thiol-terminated SAM and nTP for forming patterns of Au on a silicon wafer [9.38]. Here, the vapor phase cocondensation of the methoxy groups of molecules of 3-mercaptopropyltrimethoxysilane (MPTMS) with the −OH-terminated surface of the wafer produces a SAM of MPTMS with exposed thiol (−SH) groups. PDMS stamps can be prepared for printing on this surface by coating them with a thin film (≈ 15 nm) of Au using conditions (thermal evaporation 1.0 nm/s; ≈ 10^{-7} torr base pressure) that yield optically smooth, uniform films without the buckling that has been observed in the past with similar systems [9.42]. Nanocracking that sometimes occurs in the films deposited in this way can be reduced or eliminated by evaporating a small amount of Ti onto the PDMS before Au deposition and/or by exposing the PDMS surface briefly to an oxygen plasma. Bringing this coated stamp into contact with the MPTMS SAM leads to the formation of sulfur–gold bonds in the regions of contact. Removing the stamp after a few seconds efficiently transfers the gold from the raised regions of the stamp (Au does not adhere to the PDMS)

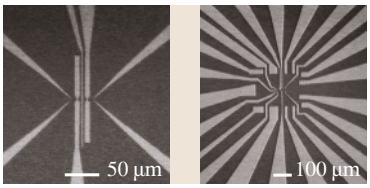

Fig. 9.11 Optical micrographs of patterns of Au (15 nm thick) formed on plastic (*left* frame) and silicon (*right* frame) substrates with nanotransfer printing. The transfer chemistries in both cases rely on self-assembled monolayers with exposed thiol groups. The minimum feature sizes and the edge resolution are both limited by the photolithography used to fabricate the stamps

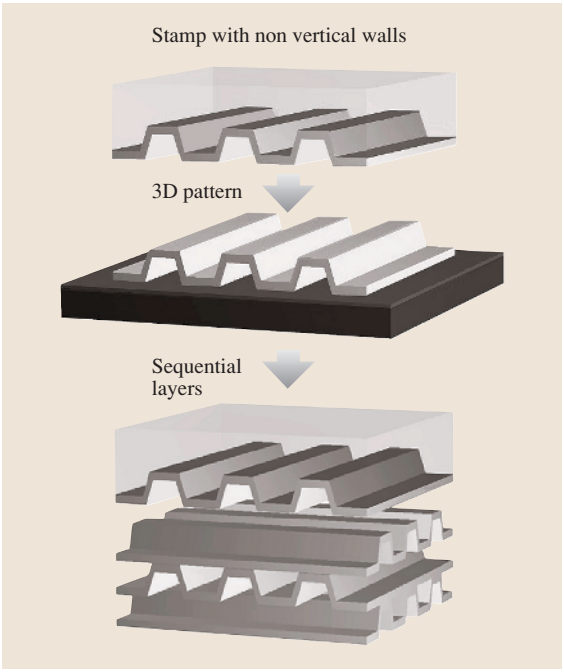

Fig. 9.12 Schematic illustration of the nanotransfer printing (nTP) process for generating continuous 3D structures when the stamp relief side walls are not vertical. Successive transfer by cold welding the gold films on top of each other yields complex multilayer structures

to the substrate. Covalent bonding of the SAM glue to both the substrate and the gold leads to good adhesion of the printed patterns: They easily pass Scotch tape adhesion tests. Similar results can be obtained with other substrates containing surface −OH groups. For example, Au patterns can be printed onto ≈ 250 µm-thick sheets of poly(ethylene terephthalate) (PET) by

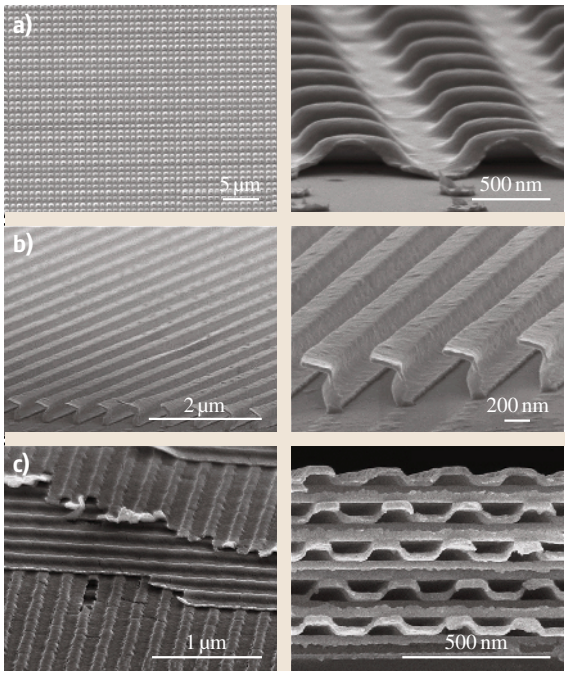

Fig. 9.13a–c Scanning electron micrographs of three-dimensional metal structures obtained by nanotransfer printing gold metal films. Part **(a)** shows closed gold nanocapsules. Part **(b)** shows free-standing *L* structures obtained using a stamp coated with a steeply angled flux of metal. Part **(c)** shows a multilayer 3-D structure obtained by the successive transfer and cold welding of continuous gold nanocorrugated films

first spin-casting and curing (130 °C for 24 h) a thin film of an organosilsesquioxane on the PET. Exposing the cured film (≈ 1 µm thick) to an oxygen plasma and then to air produces the necessary surface (−OH) groups. Figure 9.11 shows some optical micrographs of typical printed patterns in this case [9.38].

Similar surface chemistries can guide transfer to other substrates. Alkanedithiols, for example, are useful for printing Au onto GaAs wafers [9.39]. Immersing these substrates (freshly etched with 37% HCl for ≈ 2 min to remove the surface oxide) in a 0.05 M solution of 1,8-octanedithiol in ethanol for 3 h produces a monolayer of dithiol on the surface. Although the chemistry of this system is not completely clear, it is generally believed that the thiol end groups bond chemically to the surface. Surface spectroscopy suggests the formation of Ga−S and As−S bonds. Contacting an Au-coated PDMS stamp with the treated substrate causes the exposed thiol endgroups to react with Au in the regions of

contact. This reaction produces permanent Au−S bonds at the stamp/substrate interface (see insets in Fig. 9.4 for idealized chemical reaction schemes). Figure 9.12 schematically illustrates how this procedure can generate continuous 3D metal patterns using stamps with nonvertical side walls. Several layers can be transferred on top of each other by successively cold-welding the different gold metal layers. Figure 9.13 shows high- and low-magnification scanning electron microscope images of nanotransfer printed single- and multi-layer 3D metal structures [9.43,44]. The integrity of these free-standing 3D metal structures is remarkable but depends critically on the careful optimization of the metal evaporation conditions and stamp & substrate surface chemistries.

9.4 Applications

Although conventional patterning techniques, such as photolithography or electron beam lithography, have the required resolution, they are not appropriate because they are expensive and generally require multiple processing steps with resists, solvents and developers that can be difficult to use with organic active materials and plastic substrates. Microcontact and nanotransfer printing are both particularly well suited for this application. They can be combined and matched with other techniques, such as ink-jet or screen printing, to form a complete system for patterning all layers in practical plastic electronic devices [9.45]. We have focused our efforts partly on unusual electronic systems such as flexible plastic circuits and devices that rely on electrodes patterned on curved objects such as microcapillaries and optical fibers. We have also explored photonic systems such as distributed feedback structures for lasers and other integrated optical elements that demand submicron features. The sections below highlight several examples in each of these areas.

9.4.1 Unconventional Electronic Systems

A relatively new direction in electronics research seeks to establish low-cost plastic materials, substrates and printing techniques for large-area flexible electronic devices, such as paper-like displays. These types of novel devices can complement those (including high-density memories and high-speed microprocessors) that are well suited to existing inorganic (such as silicon) electronics technologies. High-resolution patterning methods for defining the separation between the source and drain electrodes (the channel length) of transistors in these plastic circuits are particularly important because this dimension determines current output and other important characteristics [9.46].

Figure 9.14 illustrates schematically a cross-sectional view of a typical organic transistor. The frame on the right shows the electrical switching characteristics of a device that uses source/drain electrodes of Au patterned by μCP, a dielectric layer of an organosilsesquioxane, a gate of indium tin oxide (ITO), and a PET substrate. The effective semiconductor mobility extracted from these data is comparable to those

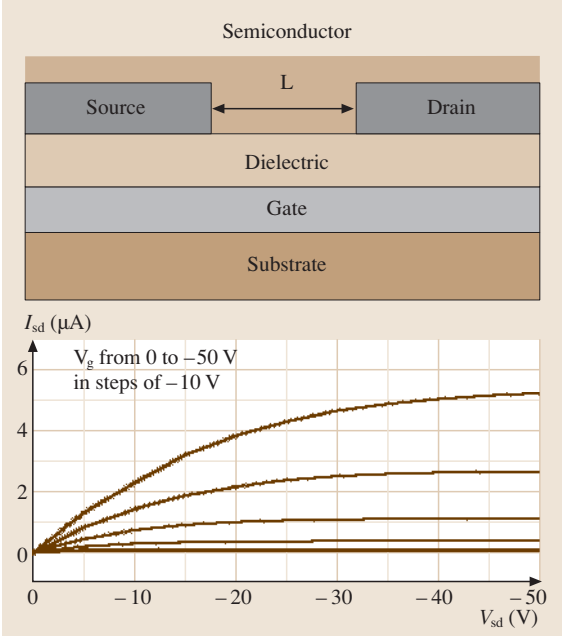

Fig. 9.14 Schematic cross-sectional view (*left*) and electrical performance (*right*) of an organic thin film transistor with microcontact printed source and drain electrodes. The structure consists of a substrate (PET), a gate electrode (indium tin oxide), a gate dielectric (spin-cast layer of organosilsesquioxane), source and drain electrodes (20 nm Au and 1.5 nm Ti), and a layer of the organic semiconductor pentacene. The electrical properties of this device are comparable to or better than those that use pentacene with photolithographically defined source/drain electrodes and inorganic dielectrics, gates and substrates

measured in devices that use the same semiconductor (pentacene in this case) with inorganic substrates and dielectrics, and gold source/drain electrodes defined by photolithography. Our recent work [9.1,31,47] with μCP in the area of plastic electronics demonstrates: (1) methods for using cylindrical "roller" stamps mounted on fixed axles for printing in a continuous reel-to-reel fashion, high-resolution source/drain electrodes in ultrathin gold and silver deposited from solution at room temperature using electroless deposition, (2) techniques for performing registration and alignment of the printed features with other elements of a circuit over large areas, (3) strategies for achieving densities of defects that are as good as those observed with photolithography when the patterning is performed outside of clean room facilities, (4) methods for removing the printed SAMs to allow good electrical contact of the electrodes with organic semiconductors deposited on top of them, and (5) materials and fabrication sequences that can efficiently exploit these printed electrodes for working organic TFTs in large-scale circuits.

Figure 9.15 provides an image of a large-area plastic circuit with critical features defined by μCP. This circuit is a flexible active matrix backplane for a display. It consists of a square array of interconnected transistors, each of which serves as a switching element that controls the color of a display pixel [9.25,48]. The transistors themselves have the layout illustrated in Fig. 9.11, and they use similar materials. The semiconductor in this image is blue (pentacene), the source/drain level is Au, the ITO appears green in the optical micrograph

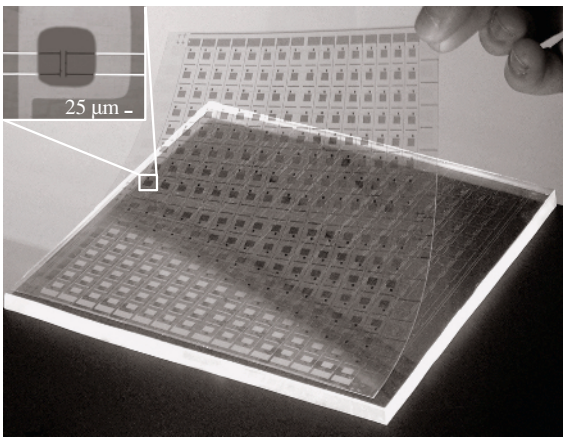

Fig. 9.15 Image of a flexible plastic active matrix backplane circuit whose finest features (transistor source/drain electrodes and related interconnects) are patterned by microcontact printing. The circuit rests partly on the elastomeric stamp that was used for printing. The circuit consists of a square array of interconnected organic transistors, each of which acts locally as a voltage-controlled switch to control the color of an element in the display. The *inset* shows an optical micrograph of one of the transistors

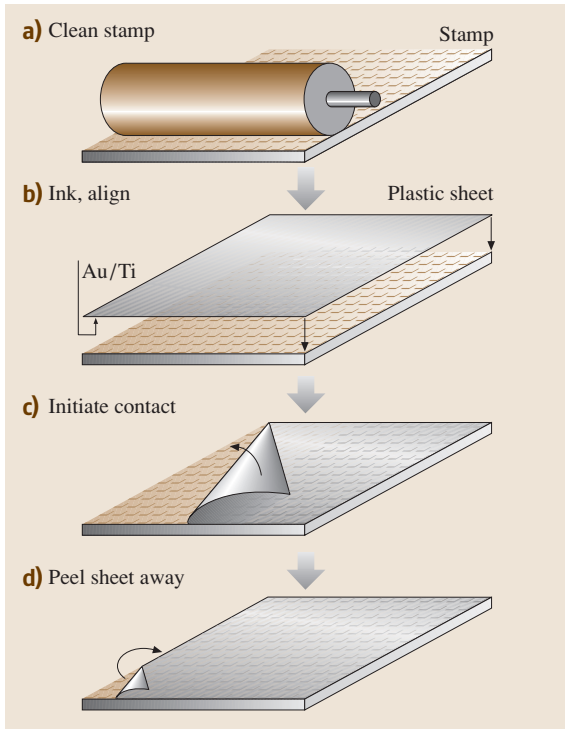

Fig. 9.16 Schematic illustration of fabrication steps for microcontact printing over large areas onto plastic sheets. The process begins with cleaning the stamp using a conventional adhesive roller lint remover. This procedure effectively removes dust particles. To minimize distortions, the stamp rests face-up on a flat surface and it is not manipulated directly during the printing. Alignment and registration are achieved with alignment marks on one side of the substrate and the stamp. By bending the plastic sheet, contact is initiated on one side of the stamp; the contact line is then allowed to progress gradually across the stamp. This approach avoids formation of air bubbles that can frustrate good contact. After the substrate is in contact with the stamp for a few seconds, the plastic substrate is separated from the stamp by peeling it away beginning in one corner. Good registration (maximum cumulative distortions of less than 50 microns over an area of 0.25 square feet) and low defect density can be achieved with this simple approach. It is also well suited for use with rigid composite stamps designed to reduce the level of distortions even further

in the inset. Part of the circuit rests on the stamp that was used for μCP. The smallest features are the source and drain electrodes (≈ 15 μm lines), the interconnecting lines (≈ 15 μm lines), and the channel length of the transistor (≈ 15 μm). This circuit incorporates five layers of material patterned with good registration of the source/drain, gate, and semiconductor levels. The simple printing approach is illustrated in Fig. 9.16 [9.25].

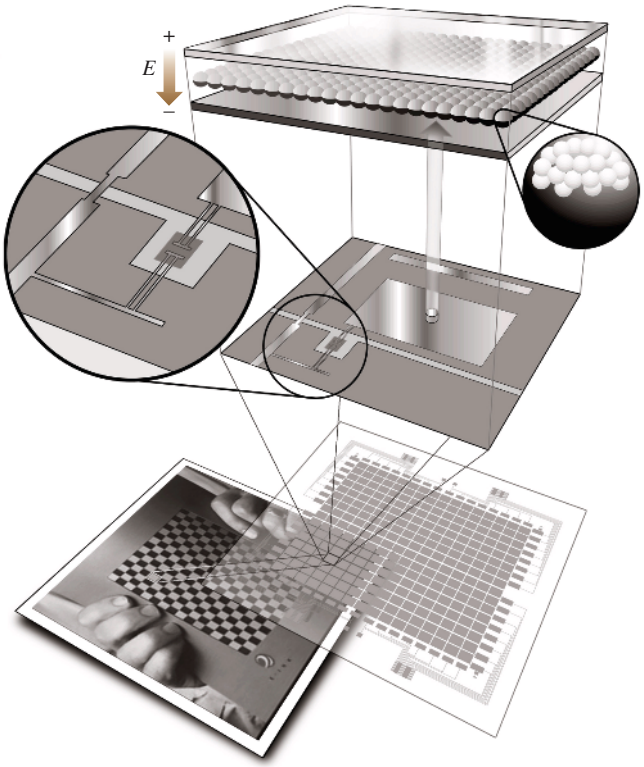

Fig. 9.17 Schematic exploded view of the components of a pixel in an electronic paperlike display (*bottom frame*) that uses a microcontact printed flexible active matrix backplane circuit (illustration near the *bottom frame*). The circuit is laminated against an unpatterned thin sheet of electronic ink (*top frame*) that consists of a monolayer of transparent polymer microcapsules (diameter ≈ 100 microns). These capsules contain a heavily dyed black fluid and a suspension of charged white pigment particles (see *right inset*). When one of the transistors turns on, electric fields develop between an unpatterned transparent frontplane electrode (indium tin oxide) and a backplane electrode that connects to the transistor. Electrophoretic flow drives the pigment particles to the front or the back of the display, depending on the polarity of the field. This flow changes the color of the pixel, as viewed from the front of the display, from black to white or vica versa

Just before use, the surface of the stamp is cleaned using a conventional adhesive roller lint remover; this procedure removes dust from the stamp in such a way that does not contaminate or damage its surface. Inking the stamp and placing it face-up on a flat surface prepares it for printing. Matching the cross-hair alignment marks on the corners of one edge of the stamp with those patterned in the ITO brings the substrate into registration with the stamp. During this alignment, features on the stamp are viewed directly through the semitransparent substrate. By bending the PET sheet, contact with the stamp is initiated on the edge of the substrate that contains the cross-hair marks. Gradually unbending the sheet allows contact to progress across the rest of the surface. This printing procedure is attractive because it avoids distortions that can arise when directly manipulating the flexible rubber stamp. It also minimizes the number and size of trapped air pockets that can form between the stamp and substrate. Careful measurements performed after etching the unprinted areas of the gold show that over the entire $6'' \times 6''$ area of the circuit, (1) the overall alignment accuracy for positioning the stamp relative to the substrate (the offset of the center of the distribution of registration errors) is ≈ 50–100 μm, even with the simple approach used here, and (2) the distortion in the positions of features in the source/drain level, when referenced to the gate level, can be as small as ≈ 50 μm (the full width at half maximum of the distribution of registration errors). These distortions represent the cumulative effects of deformations in the stamp and distortions in the gate and column electrodes that may arise during the patterning and processing of the flexible PET sheet. The density of defects in the printed patterns is comparable to (or smaller than) that in resist patterned by contact-mode photolithography when both procedures are performed outside of a clean-room facility (when dust is the dominant source of defects).

Figure 9.17 shows an "exploded" view of a paperlike display that consists of a printed flexible plastic backplane circuit, like the one illustrated in Fig. 9.16, laminated against a thin layer of "electronic ink" [9.25, 49]. The electronic ink is composed of a monolayer of transparent polymer microcapsules that contain a suspension of charged white pigment particles suspended in a black liquid. The printed transistors in the backplane circuit act as local switches, which control electric fields that drive the pigments to the front or back of the display. When the particles flow to the front of a microcapsule, it appears white; when they flow to the back, it appears black. Figure 9.18 shows a working sheet of active matrix electronic paper that uses this design.

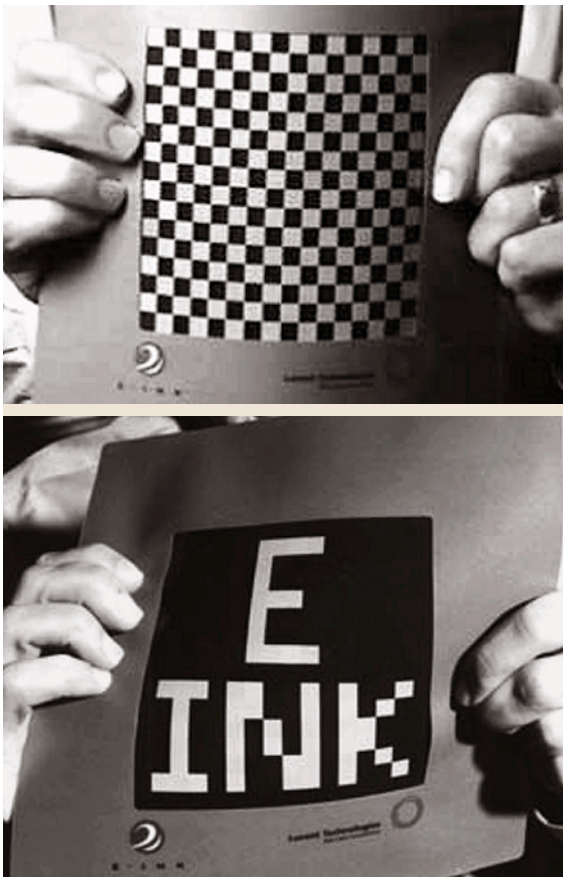

Fig. 9.18 Electronic paperlike display showing two different images. The device consists of several hundred pixels controlled by a flexible active matrix backplane circuit formed by microcontact printing. The relatively coarse resolution of the display is not limited by material properties or by the printing techniques. Instead, it is set by practical considerations for achieving high pixel yields in the relatively uncontrolled environment of the chemistry laboratory in which the circuits were fabricated

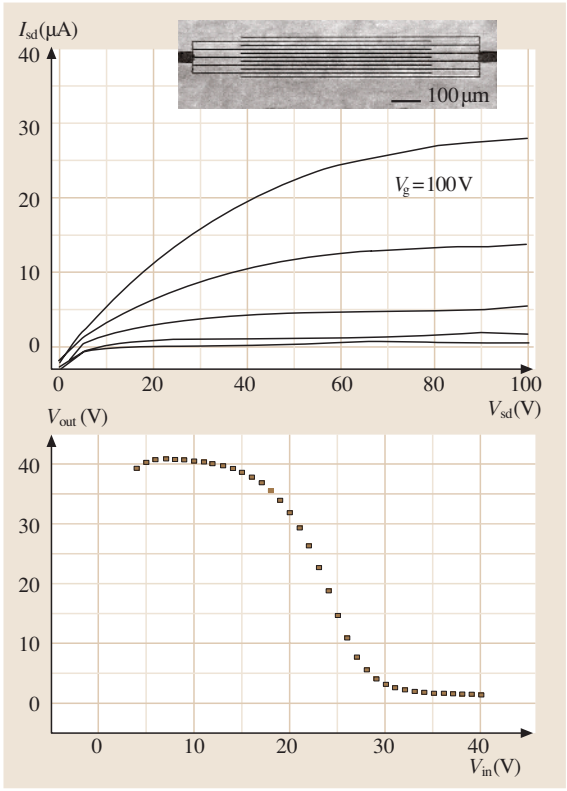

Fig. 9.19 The *upper* frame shows current–voltage characteristics of an n-channel transistor formed with electrodes patterned by nanotransfer printing that are laminated against a substrate that supports an organic semiconductor, a gate dielectric and a gate. The *inset* shows an optical micrograph of the interdigitated electrodes. The *lower* frame shows the transfer characteristics of a simple CMOS inverter circuit that uses this device and a similar one for the p-channel transistor

This prototype display has several hundred pixels and an optical contrast that is both independent of the viewing angle and significantly better than newsprint. The device is ≈ 1 mm thick, is mechanically flexible, and weighs ≈ 80% less than a conventional liquid crystal display of similar size. Although these displays have only a relatively coarse resolution, all of the processing techniques, the μCP method, the materials, and the electronic inks, are suitable for the large numbers of pixels required for high-information content electronic newspapers and other systems.

Like μCP, nTP is well suited to forming high-resolution source/drain electrodes for plastic electronics. nTP of Au/Ti features in the geometry of the drain and source level of organic transistors, and with appropriate interconnects on a thin layer of PDMS on PET it yields a substrate that can be used in an unusual but powerful way for building circuits: soft, room temperature lamination of such a structure against a plastic substrate that supports the semiconductor, gate dielectric, and gate levels yields a high performance circuit embedded between two plastic sheets [9.37,50]. (Details of this lamination procedure are presented elsewhere.) The left frame of Fig. 9.19 shows the current–voltage characteristics of a laminated n-channel transistor that uses the

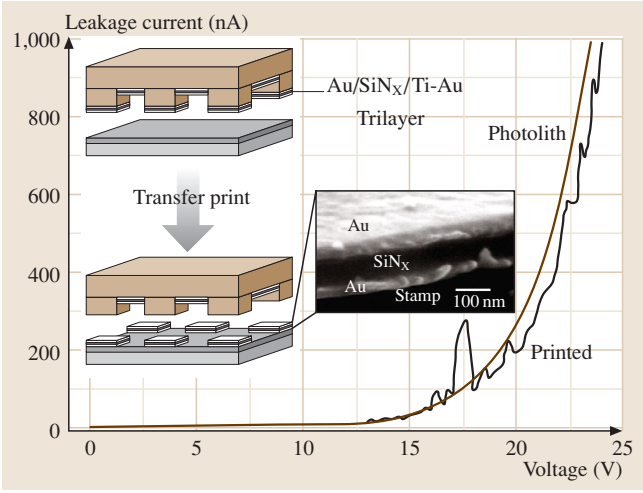

Fig. 9.20 Multilayer thin film capacitor structure printed in a single step onto a plastic substrate using the nanotransfer printing technique. A multilayer of Au/SiN – x/Ti/Au was first deposited onto a silicon stamp formed by photolithography and etching. Contacting this stamp to a substrate of Au/PDMS/PET forms a cold weld that bonds the exposed Au on the stamp to the Au-coating on the substrate. Removing the stamp produces arrays of square (250 mm × 250 mm) metal/insulator/metal capacitors on the plastic support. The *dashed line* shows the measured current–voltage characteristics of one of these printed capacitors. The *solid line* corresponds to a similar structure formed on a rigid glass substrate using conventional photolithographic procedures. The characteristics are the same for these two cases. The slightly higher level of noise in the printed devices results, at least partly, from the difficulties involved with making good electrical contacts to structures on the flexible plastic substrate

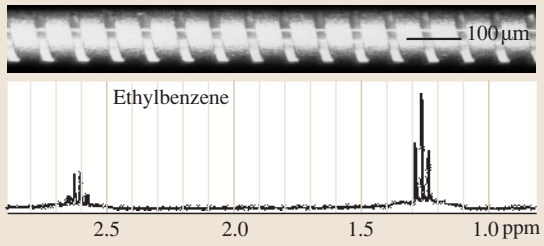

Fig. 9.21 The *top frame* shows an optical micrograph of a continuous conducting microcoil formed by microcontact printing onto a microcapillary tube. This type of printed microcoil is well suited for excitation and detection of nuclear magnetic resonance spectra from nanoliter volumes of fluid housed in the bore of the microcapillary. The *bottom frame* shows a spectra trace collected from an ≈ 8 nL volume of ethyl benzene using a structure similar to the one shown in the *top frame*

organic semiconductor copper hexadecafluorophthalocyanine (n-type) and source/drain electrodes patterned with nTP. The inset shows an optical micrograph of the printed interdigitated source/drain electrodes of this device. The bottom frame of Fig. 9.16 shows the transfer characteristics of a laminated complementary organic inverter circuit whose electrodes and connecting lines are defined by nTP. The p-channel transistor in this circuit used pentacene for the semiconductor [9.37].

In addition to high-resolution source/drain electrodes, it is possible to use nTP to form complex multilayer devices with electrical functionality on plastic substrates [9.38]. Figure 9.20 shows a metal/insulator/metal (MIM) structure of Au (50 nm), SiN_x (100 nm; by plasma enhanced vapor deposition, PECVD), Ti (5 nm) and Au (50 nm) formed by transfer printing with a silicon stamp that is coated sequentially with these layers. In this case, a short reactive ion etch (with CF_4) after the second Au deposition removes the SiN_x from the sidewalls of the stamp. nTP transfers these layers in a patterned geometry to a substrate of Au(15 nm)/Ti(1 nm)-coated PDMS(50 µm)/PET(250 µm). Interfacial cold-welding between the Au on the surfaces of the stamp and substrate bonds the multilayers to the substrate. Figure 9.8 illustrates the procedures, the structures (lateral dimensions of 250 µm × 250 µm, for ease of electrical probing), and their electrical characteristics. These MIM capacitors have performances similar to devices fabricated on silicon wafers by photolithography and lift-off. This example illustrates the ability of nTP to print patterns of materials whose growth conditions (high-temperature SiN_x by PECVD, in this case) prevent their direct deposition or processing on the substrate of interest (PET, in this case). The cold-welding transfer approach has also been exploited in other ways for patterning components for plastic electronics [9.51, 52].

Another class of unusual electronic/optoelectronic devices relies on circuits or circuit elements on curved surfaces. This emerging area of research was stimulated primarily by the ability of µCP to print high-resolution features on fibers and cylinders. Figure 9.21 shows a conducting microcoil printed with µCP on a microcapillary tube using the approach illustrated in Fig. 9.4. The coil serves as the excitation and detection element for high-resolution proton nuclear magnetic resonance of nanoliter volumes of fluid that are housed in the bore of the microcapillary [9.53]. The high fill factor and other considerations lead to extremely high sensitiv-

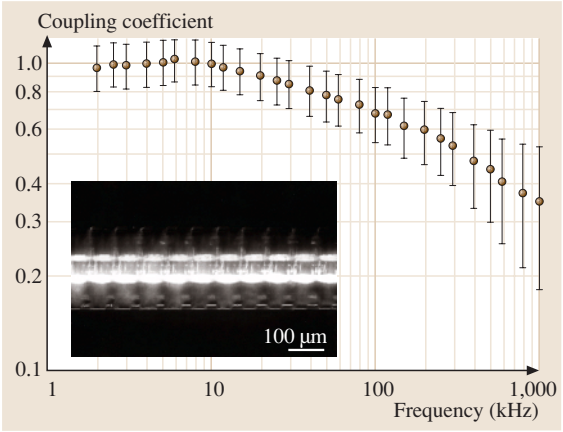

Fig. 9.22 The *inset* shows a concentric microtransformer formed using microcoils printed onto two different microcapillary tubes. The smaller of the tubes (outer diameter 135 microns) has a ferromagnetic wire threaded through its core. The larger one (outer diameter 350 microns) has the smaller tube threaded through its core. The resulting structure is a microtransformer that shows good coupling coefficients at frequencies up to ≈ 1 MHz. The graph shows its performance

ity with such printed coils. The bottom frame of Fig. 9.21 shows the spectrum of an ≈ 8 nL volume of ethylbenzene. The narrow lines demonstrate the high resolution that is possible with this approach. Similar coils can be used as magnets [9.54], springs [9.36], and electrical transformers [9.55]. Figure 9.22 shows an optical micrograph and the electrical measurements from a concentric cylindrical microtransformer that uses a microcoil printed on a microcapillary tube with a ferromagnetic wire threaded through its core. Inserting this structure into the core of a larger microcapillary that also supports a printed microcoil completes the transformer [9.55]. This type of device shows good coupling coefficients up to relatively high frequencies. Examples of other optoelectronic components appear in fiber optics where microfabricated on-fiber structures serve as integrated photomasks [9.20] and distributed thermal actuators [9.22].

9.4.2 Lasers and Waveguide Structures

In addition to integral components of unconventional electronic systems, useful structures for integrated optics can be built by using μCP and nTP to print sacrificial resist layers for etching glass waveguides. These printing techniques offer the most significant potential

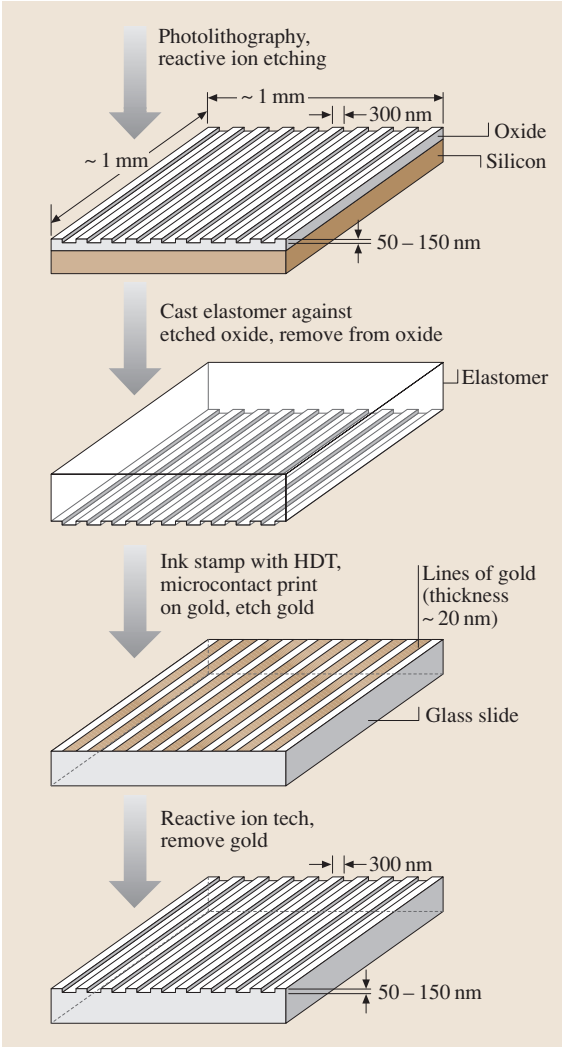

Fig. 9.23 Schematic illustration of the use of microcontact printing (μCP) for fabricating high-resolution gratings that can be incorporated into distributed planar laser structures or other components for integrated optics. The geometries illustrated here are suitable for third- order distributed feedback (DFB) lasers that operate in the red

value for this area when they are used to pattern features that are smaller than those that can be achieved with contact mode photolithography. Mode coupling gratings and distributed laser resonators are two such classes of structures. We have demonstrated μCP for forming distributed feedback (DFB) and distributed Bragg reflector (DBR) lasers that have narrow emission line widths [9.56]. This challenging fabrication

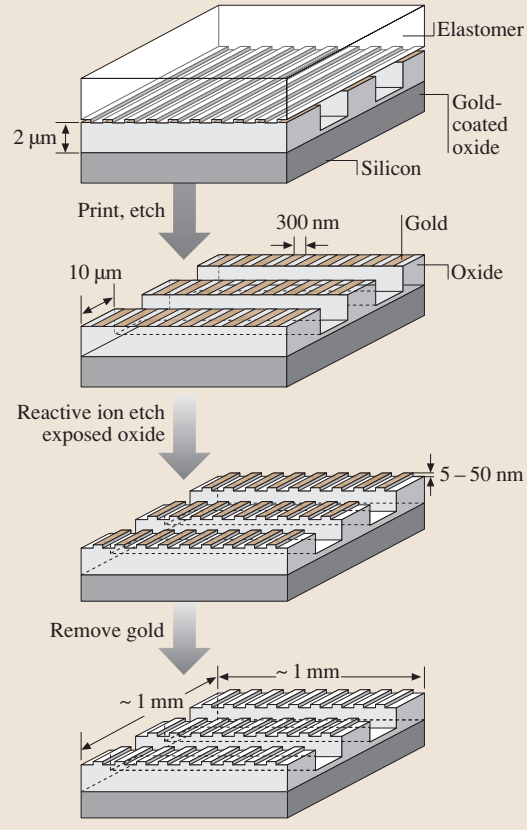

Fig. 9.24 The *top frames* gives a schematic illustration of steps for microcontact printing high-resolution gratings directly onto the top surfaces of ridge waveguides. The printing defines a sacrificial etch mask of gold which is subsequently removed. Producing this type of structure with photolithography is difficult because of severe thickness nonuniformities that appear in photoresist spin-cast on this type of nonplanar substrate. The *upper bottom* frame shows a top view optical micrograph of printed gold lines on the ridge waveguides. The *lower bottom* frame shows the emission output of a plastic photopumped laser that uses the printed structure and a thin evaporated layer of gain media

demonstrates the suitability of μCP for building structures that have (1) feature sizes of significantly less than one micron (≈ 300 nm), *and* (2) long-range spatial coherence (≈ 1 mm). The lasers employ optically pumped gain material deposited onto DFB or DBR resonators formed from periodic relief on a transparent substrate. The gain media confines light to the surface of the structure; its thickness is chosen to support a single transverse mode. To generate the required relief, lines of gold formed by μCP on a glass slide act as resists for reactive ion etching of the glass. Removing the gold leaves a periodic pattern of relief (600 nm period, 50 nm depth) on the surface of the glass (see Fig. 9.23). Figure 9.24 shows the performance of plastic lasers that use printed DFB and DBR resonators with gain media consisting of thin films of PBD doped with 1% by weight of coumarin 490 and DCMII, photopumped with 2 ns pulses from a nitrogen laser with intensities $> 5\,\mathrm{kW/cm^2}$ [9.56]. Multimode lasing at resolution-limited line widths was observed at wavelengths corresponding to the third harmonic of the gratings. These characteristics are similar to those observed in lasers that use resonators generated with photolithography and are better than those that use imprinted polymers [9.57].

Contact printing not only provides a route to low-cost equivalents of gratings fabricated with other approaches, but also allows the fabrication of structures that would be difficult or impossible to generate with photolithography. For example, μCP can be used to form DFB resonators directly on the top surfaces of ridge waveguides [9.58]. Figure 9.25 illustrates the procedures. The bottom left frame shows an optical micrograph of the printed gold lines. Sublimation of a ≈ 200 nm film of tris(8-hydroxyquinoline) aluminium (Alq) doped with 0.5–5.0 weight percent of the laser dye DCMII onto the resonators produces waveguide DFB lasers. The layer of

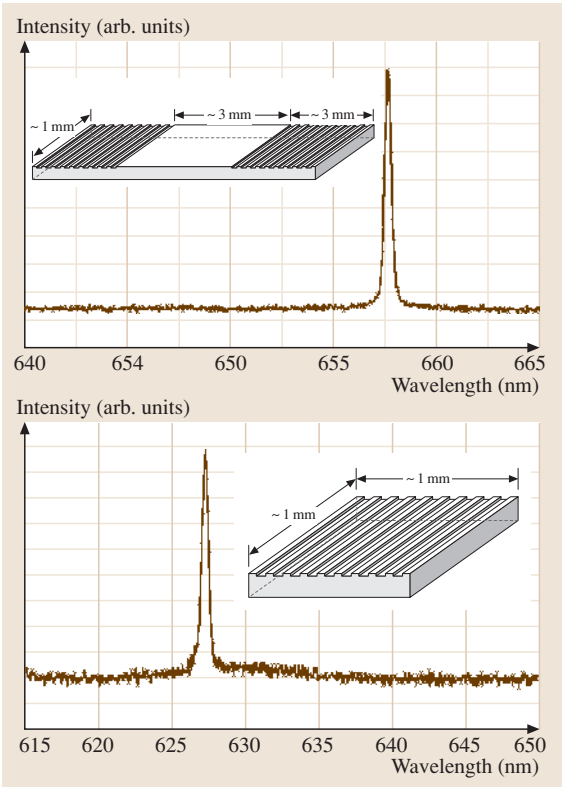

Fig. 9.25 Schematic illustrations and lasing spectra of plastic lasers that use microcontact printed resonators based on surface relief distributed Bragg reflectors (DBRs) and distributed feedback gratings (DFBs) on glass substrates. The grating periods are ≈ 600 nm in both cases. The lasers use thin film plastic gain media deposited onto the printed gratings. This layer forms a planar waveguide that confines the light to the surface of the substrate. The laser shows emission over a narrow wavelength range, with a width that is limited by the resolution of the spectrometer used to characterize the output. In both cases, the emission profiles, the lasing thresholds and other characteristics of the devices are comparable to similar lasers that use resonators formed by high-resolution projection-mode photolithography

gain material itself provides a planar waveguide with air and polymer as the cladding layers. The relief waveguide provides lateral confinement of the light. Photopumping these devices with the output of a pulsed nitrogen laser (≈ 2 ns, 337 nm) causes lasing due to Bragg reflections induced by the DFB structures on the top surfaces of the ridge waveguides. Some of the laser emission scatters out of the plane of the waveguide at an angle allowed by phase matching conditions. In this way, the grating also functions as an output coupler and offers a convenient way to characterize the laser emission. The bottom right frame of Fig. 9.22 shows the emission profile.

9.5 Conclusions

This chapter provides an overview of two contact printing techniques that are capable of micron and submicron resolution. It also illustrates some applications of these methods that may provide attractive alternatives to more established lithographic methods. The growing interest in nanoscience and technology makes it crucial to develop new methods for fabricating the relevant test structures and devices. The simplicity of these techniques together with the interesting and subtle materials science, chemistry, and physics associated with them make this a promising area for basic and applied study.

References

9.1 C. A. Mirkin, J. A. Rogers: Emerging methods for micro- and nanofabrication, MRS Bull. **26**, 506–507 (2001)

9.2 H. I. Smith, H. G. Craighead: Nanofabrication, Phys. Today **43**, 24–43 (February 1990)

9.3 W. M. Moreau (Ed.): *Semiconductor Lithography: Principles and Materials* (Plenum, New York 1988)

9.4 S. Matsui, Y. Ochiai: Focused ion beam applications to solid state devices, Nanotechnology **7**, 247–258 (1996)

9.5 J. M. Gibson: Reading and writing with electron beams, Phys. Today **50**, 56–61 (1997)

9.6 L. L. Sohn, R. L. Willett: Fabrication of nanostructures using atomic-force microscope-based lithography, Appl. Phys. Lett. **67**, 1552–1554 (1995)

9.7 E. Betzig, K. Trautman: Near-field optics – microscopy, spectroscopy, and surface modification beyond the diffraction limit, Science **257**, 189–195 (1992)

9.8 A. J. Bard, G. Denault, C. Lee, D. Mandler, D. O. Wipf: Scanning electrochemical microscopy: a new technique for the characterization and modification of surfaces, Acc. Chem. Res. **23**, 357 (1990)

9.9 J. A. Stroscio, D. M. Eigler: Atomic and molecular manipulation with the scanning tunneling microscope, Science **254**, 1319–1326 (1991)

9.10 J. Nole: Holographic lithography needs no mask, Laser Focus World **33**, 209–212 (1997)

9.11 A. N. Broers, A. C. F. Hoole, J. M. Ryan: Electron beam lithography – resolution limits, Microelectron. Eng. **32**, 131–142 (1996)

9.12 A. N. Broers, W. Molzen, J. Cuomo, N. Wittels: Electron-beam fabrication of 80 Å metal structures, Appl. Phys. Lett. **29**, 596 (1976)

9.13 G. D. Aumiller, E. A. Chandross, W. J. Tomlinson, H. P. Weber: Submicrometer resolution replication of relief patterns for integrated optics, J. Appl. Phys. **45**, 4557–4562 (1974)

9.14 Y. Xia, J. J. McClelland, R. Gupta, D. Qin, X.-M. Zhao, L. L. Sohn, R. J. Celotta, G. M. Whiteside: Replica molding using polymeric materials: a practical step toward nanomanufacturing, Adv. Mater. **9**, 147–149 (1997)

9.15 T. Borzenko, M. Tormen, G. Schmidt, L. W. Molenkamp, H. Janssen: Polymer bonding process for nanolithography, Appl. Phys. Lett. **79**, 2246–2248 (2001)

9.16 H. Hua, Y. Sun, A. Gaur, M. A. Meitl, L. Bilhaut, L. Rotinka, J. Wang, P. Geil, M. Shim, J. A. Rogers: Polymer imprint lithography with molecular-scale resolution, Nano Lett. **4(12)**, 2467–2471 (2004)

9.17 A. Kumar, G. M. Whitesides: Features of gold having micrometer to centimeter dimensions can be formed through a combination of stamping with an elastomeric stamp and an alkanethiol ink followed by chemical etching, Appl. Phys. Lett. **63**, 2002–2004 (1993)

9.18 Y. Xia, G. M. Whitesides: Soft lithography, Angew. Chem. Int. Ed. **37**, 550–575 (1998)

9.19 Y. Xia, J. A. Rogers, K. E. Paul, G. M. Whitesides: Unconventional methods for fabricating and patterning nanostructures, Chem. Rev. **99**, 1823–1848 (1999)

9.20 J. A. Rogers, R. J. Jackman, J. L. Wagener, A. M. Vengsarkar, G. M. Whitesides: Using microcontact printing to generate photomasks on the surface of optical fibers: a new method for producing in-fiber gratings, Appl. Phys. Lett. **70**, 7–9 (1997)

9.21 B. Michel, A. Bernard, A. Bietsch, E. Delamarche, M. Geissler, D. Juncker, H. Kind, J. P. Renault, H. Rothuizen, H. Schmid, P. Schmidt-Winkel, R. Stutz, H. Wolf: Printing meets lithography: soft approaches to high-resolution printing, IBM J. Res. Dev. **45**, 697–719 (2001)

9.22 J. A. Rogers: Rubber stamping for plastic electronics and fiber optics, MRS Bull. **26**, 530–534 (2001)

9.23 N. B. Larsen, H. Biebuyck, E. Delamarche, B. Michel: Order in microcontact printed self-assembled monolayers, J. Am. Chem. Soc. **119**, 3017–3026 (1997)

9.24 H. A. Biebuyck, G. M. Whitesides: Self-organization of organic liquids on patterned self-assembled monolayers of alkanethiolates on gold, Langmuir **10**, 2790–2793 (1994)

9.25 J. A. Rogers, Z. Bao, K. Baldwin, A. Dodabalapur, B. Crone, V. R. Raju, V. Kuck, H. Katz, K. Amundson, J. Ewing, P. Drzaic: Paper-like electronic displays: Large area, rubber stamped plastic sheets of electronics and electrophoretic inks, Proc. Nat. Acad. Sci. USA **98**, 4835–4840 (2001)

9.26 J. L. Wilbur, H. A. Biebuyck, J. C. MacDonald, G. M. Whitesides: Scanning force microscopies can image patterned self-assembled monolayers, Langmuir **11**, 825–831 (1995)

9.27 J. C. Love, D. B. Wolfe, M. L. Chabinyc, K. E. Paul, G. M. Whitesides: Self-assembled monolayers of alkanethiolates on palladium are good etch resists, J. Am. Chem. Soc. **124**, 1576–1577 (2002)

9.28 H. Schmid, B. Michel: Siloxane polymers for high-resolution, high-accuracy soft lithography, Macromolecules **33**, 3042–3049 (2000)

9.29 K. Choi, J. A. Rogers: A photocurable poly(dimethylsiloxane) chemistry for soft lithography in the nanometer regime, J. Am. Chem. Soc. **125**, 4060–4061 (2003)

9.30 J. A. Rogers, K. E. Paul, G. M. Whitesides: Quantifying distortions in soft lithography, J. Vacuum. Sci. Tech. B **16**, 88–97 (1998)

9.31 J. Tate, J. A. Rogers, C. D. W. Jones, W. Li, Z. Bao, D. W. Murphy, R. E. Slusher, A. Dodabalapur, H. E. Katz, A. J. Lovinger: Anodization and microcontact printing on electroless silver: solution-based fabrication procedures for low voltage organic electronic systems, Langmuir **16**, 6054–6060 (2000)

9.32 Y. Xia, E. Kim, G. M. Whitesides: Microcontact printing of alkanethiols on silver and its application to microfabrication, J. Electrochem. Soc. **143**, 1070–1079 (1996)

9.33 Y. N. Xia, X. M. Zhao, E. Kim, G. M. Whitesides: A selective etching solution for use with patterned self-assembled monolayers of alkanethiolates on gold, Chem. Mater. **7**, 2332–2337 (1995)

9.34 R. J. Jackman, J. Wilbur, G. M. Whitesides: Fabrication of submicrometer features on curved substrates by microcontact printing, Science **269**, 664–666 (1995)

9.35 R. J. Jackman, S. T. Brittain, A. Adams, M. G. Prentiss, G. M. Whitesides: Design and fabrication of topologically complex, three-dimensional microstructures, Science **280**, 2089–2091 (1998)

9.36 J. A. Rogers, R. J. Jackman, G. M. Whitesides: Microcontact printing and electroplating on curved substrates: a new means for producing free-standing three-dimensional microstructures with possible

applications ranging from micro-coil springs to coronary stents, Adv. Mater. **9**, 475–477 (1997)
9.37 Y.-L. Loo, R. W. Willett, K. Baldwin, J. A. Rogers: Additive, nanoscale patterning of metal films with a stamp and a surface chemistry mediated transfer process: applications in plastic electronics, Appl. Phys. Lett. **81**, 562–564 (2002)
9.38 Y.-L. Loo, R. W. Willett, K. Baldwin, J. A. Rogers: Interfacial chemistries for nanoscale transfer printing, J. Am. Chem. Soc. **124**, 7654–7655 (2002)
9.39 Y.-L. Loo, J. W. P. Hsu, R. L. Willett, K. W. Baldwin, K. W. West, J. A. Rogers: High-resolution transfer printing on GaAs surfaces using alkane dithiol self-assembled monolayers, J. Vacuum. Sci. Tech. B. **20**, 2853–2856 (2002)
9.40 G. S. Ferguson, M. K. Chaudhury, G. B. Sigal, G. M. Whitesides: Contact adhesion of thin gold-films on elastomeric supports – cold welding under ambient conditions, Science **253**, 776–778 (1991)
9.41 W. Zhang, S. Y. Chou: Multilevel nanoimprint lithography with submicron alignment over 4 in Si wafers, Appl. Phys. Lett. **79**, 845–847 (2001)
9.42 N. Bowden, S. Brittain, A. G. Evans, J. W. Hutchinson, G. M. Whitesides: Spontaneous formation of ordered structures in thin films of metals supported on an elastomeric polymer, Nature **393**, 146–149 (1998)
9.43 E. Menard, L. Bilhaut, J. Zaumseil, J. A. Rogers: Improved surface chemistries, thin film deposition techniques, and stamp designs for nanotransfer printing, Langmuir **20**, 6871–6878 (2004)
9.44 J. Zaumseil, M. A. Meitl, J. W. P. Hsu, B. Acharya, K. W. Baldwin, Y.-L. Loo, J. A. Rogers: Three-dimensional and multilayer nanostructures formed by nanotransfer printing, Nano. Lett. **3**, 1223–1227 (2003)
9.45 Z. Bao, J. A. Rogers, H. E. Katz: Printable organic and polymeric semiconducting materials and devices, J. Mater. Chem. **9**, 1895–1904 (1999)
9.46 J. A. Rogers, Z. Bao, A. Dodabalapur, A. Makhija: Organic smart pixels and complementary inverter circuits formed on plastic substrates by casting, printing and molding, IEEE Electron Dev. Lett. **21**, 100–103 (2000)
9.47 J. A. Rogers, Z. Bao, A. Makhija: Non-photolithographic fabrication sequence suitable for reel-to-reel production of high performance organic transistors and circuits that incorporate them, Adv. Mater. **11**, 741–745 (1999)
9.48 P. Mach, S. Rodriguez, R. Nortrup, P. Wiltzius, J. A. Rogers: Active matrix displays that use printed organic transistors and polymer dispersed liquid crystals on flexible substrates, Appl. Phys. Lett. **78**, 3592–3594 (2001)
9.49 J. A. Rogers: Toward paperlike displays, Science **291**, 1502–1503 (2001)
9.50 Y.-L. Loo, T. Someya, K. W. Baldwin, P. Ho, Z. Bao, A. Dodabalapur, H. E. Katz, J. A. Rogers: Soft, conformable electrical contacts for organic transistors: high resolution circuits by lamination, Proc. Nat. Acad. Sci. USA **99**, 10252–10256 (2002)
9.51 C. Kim, P. E. Burrows, S. R. Forrest: Micropatterning of organic electronic devices by cold-welding, Science **288**, 831–833 (2000)
9.52 C. Kim, M. Shtein, S. R. Forrest: Nanolithography based on patterned metal transfer and its application to organic electronic devices, Appl. Phys. Lett. **80**, 4051–4053 (2002)
9.53 J. A. Rogers, R. J. Jackman, G. M. Whitesides, D. L. Olson, J. V. Sweedler: Using microcontact printing to fabricate microcoils on capillaries for high resolution ^{1}H-NMR on nanoliter volumes, Appl. Phys. Lett. **70**, 2464–2466 (1997)
9.54 J. A. Rogers, R. J. Jackman, G. M. Whitesides: Constructing single and multiple helical microcoils and characterizing their performance as components of microinductors and microelectromagnets, J. Microelectromech. Sys. (JMEMS) **6**, 184–192 (1997)
9.55 R. J. Jackman, J. A. Rogers, G. M. Whitesides: Fabrication and characterization of a concentric, cylindrical microtransformer, IEEE Trans. Magn. **33**, 2501–2503 (1997)
9.56 J. A. Rogers, M. Meier, A. Dodabalapur: Using stamping and molding techniques to produce distributed feedback and Bragg reflector resonators for plastic lasers, Appl. Phys. Lett. **73**, 1766–1768 (1998)
9.57 M. Berggren, A. Dodabalapur, R. E. Slusher, A. Timko, O. Nalamasu: Organic solid-state lasers with imprinted gratings on plastic substrates, Appl. Phys. Lett. **72**, 410–411 (1998)
9.58 J. A. Rogers, M. Meier, A. Dodabalapur: Distributed feedback ridge waveguide lasers fabricated by nanoscale printing and molding on nonplanar substrates, Appl. Phys. Lett. **74**, 3257–3259 (1999)